



F. Jiang
Z. Xia
S. Li
G. Eckert
J. Chen

Mechanical environment change in root, periodontal ligament, and alveolar bone in response to two canine retraction treatment strategies

Authors' affiliations:

F. Jiang, S. Li, J. Chen, Department of Mechanical Engineering, Indiana University-Purdue University, Indianapolis, IN, USA

Z. Xia, Shenzhen Institutes of Advanced Technology, Chinese Academy of Sciences, Chinese University of Hong Kong, Hong Kong, China

G. Eckert, Department of Biostatistics, Indiana University, Indianapolis, IN, USA

Correspondence to:

J. Chen

Department of Mechanical Engineering
Indiana University-Purdue University
Indianapolis, 723 W Michigan St, SL260
Indianapolis, IN 46202
USA

E-mail: jchen3@iupui.edu

Jiang F., Xia Z., Li S., Eckert G., Chen J. Mechanical environment change in root, periodontal ligament, and alveolar bone in response to two canine retraction treatment strategies

Orthod Craniofac Res 2015; **18**(Suppl. 1): 29–38. © 2015 John Wiley & Sons A/S. Published by John Wiley & Sons Ltd

Structured Abstract

Objective – To investigate the initial mechanical environment (ME) changes in root surface, periodontal ligament (PDL), and alveolar bone due to two treatment strategies, low or high moment-to-force ratio (M/F).

Setting and Sample Population – Indiana University-Purdue University Indianapolis. Eighteen patients who underwent maxillary bilateral canine retraction.

Material and method – Finite element models of the maxillary canines from the patients were built based on their cone beam computed tomography scans. For each patient, the canine on one side had a specially designed T-loop spring with the M/F higher than the other side. Four stress invariants (1st principal/dilatational/3rd principal/von Mises stress) in the tissues were calculated. The stresses were compared with the bone mineral density (BMD) changes reported previously for linking the ME change to bone modeling/remodeling activities. The correlation was tested by the mixed-model ANOVA.

Results – The alveolar bone in the direction of tooth movement is primarily in tension, while the PDL is in compression; the stresses in the opposite direction have a reversed pattern. The M/F primarily affects the stress in root. Three stress invariants (1st principal/3rd principal/dilatational stress) in the tooth movement direction have moderate correlations with BMD loss.

Conclusions – The stress invariants may be used to characterize what the osteocytes sense when ME changes. Their distributions in the tissues are significantly different, meaning the cells experience different stimuli. The higher bone activities along the direction of tooth movement may be related to the initial volumetric increase and decrease in the alveolar bone.

Key words: canine retraction; finite element analysis; mechanotransduction

Date:

Accepted 11 December 2014

DOI: 10.1111/ocr.12076

© 2015 John Wiley & Sons A/S.
Published by John Wiley & Sons Ltd

Introduction

Orthodontic tooth movement is both pathologic and physiologic in response to orthodontic load (1). When an orthodontic load is applied to a tooth, the periodontal ligament (PDL) is compressed in front of the root and stretched on the back, which results in mechanical environment (ME) changes in the alveolar bone. The change of ME in terms of stress and strain triggers the biological reaction. Osteoclasts are recruited and absorb the bone in front of the tooth in the moving direction (2, 3). Osteoblasts are recruited on the opposite side to form new bone (2). This modeling and remodeling process results in tooth translocation and is reflected by the bone mineral density (BMD) change.

A mechanical stimulus is one of the determination factors to the number and activity of osteoclasts and osteoblasts, and other factors, such as hormones and cytokines, are also influential and patient dependent (4–6). The osteocyte is commonly believed to be a source of soluble factors targeting cells on bone surface and distant organs (7). It is embedded within the calcified bone matrix, and likely to be responsible for sensing the mechanical stimuli and regulating bone formation and resorption (8). Mechanically activated osteocytes have the function to modulate the recruitment, differentiation, and activity of osteoblasts and osteoclasts (6, 9–11).

The questions remain as how the cells are triggered; whether the mechanotransduction process is initiated in bone or PDL; and whether the resulting bone modeling/remodeling characterized by the BMD changes are predominantly determined by the initial stress due to orthodontic load. The answers to the questions help understand the root cause of the tooth movement, which require study of ME changes due to orthodontic treatment.

While orthodontists try to control the tooth movement and root resorption, it will be beneficial to understand how biological tissues respond to the ME changes. Heavy force causes more root resorption (12, 13). Compressive stress in PDL is reported to be related to the root resorption in an animal study (14). Clinical stud-

ies had shown the correlation between movement direction and BMD loss (15, 16). However, to understand the root cause, it is important to understand how the cells sense the ME changes in different tissues.

The objectives of this study were to study the initial stress in the root surface, PDL, and alveolar bone to help understand the kind of stimuli the cell may experience within these tissues and the effects of initial M/F on the ME changes. As one example, the correlation between the stress and the BMD in terms of Hounsfield Unit (HU) change in the surrounding alveolar bone is evaluated to understand the possible stimuli causing the HU reduction.

Material and methods

Eighteen patients (seven males and 11 females) who underwent maxillary bilateral canine retraction as a part their orthodontic treatments were involved in this study. The average age was 19 ± 9 years old. The study was approved by the Indiana University Institutional Review Board.

For each patient, the centers of resistance of the two maxillary canines were calculated using finite element (FE) method (17). The canine on one side was under translation (TR) treatment and the other side was under controlled tipping (CT), which were assigned randomly and accomplished by patient-specific custom-designed segmental T-loops. The T-loop delivered approximately 125 cN of closing force with desired M/F for TR or CT (17). The M/F for TR was higher than for CT.

The cone beam computed tomography (CBCT) scans were taken before and after canine retraction for each patient. The average time for canine retraction was 4.9 months which varied depending on the size of the initial space, patients' appliance on appointment, and inter-patient variations. The canines displaced on average 2.1 ± 1.5 mm (18).

The FE model consisted of the crown, root, PDL, and alveolar bone. The alveolar bone had both cancellous bone and a thin layer of cortical bone (19). The PDL was modeled as a fiber-rein-

forced structure (20). The fibers resisted tensile forces only.

The geometry of a canine was obtained from each patient's CBCT images. MIMICS (Materialise, Leuven, Belgium), image processing software, and Pro-E (PTC Inc., Needham, MA, USA), computer-aided design software, were used to create the FE model. The thickness of human PDL is reported to be around 0.1–0.3 mm (0.2 mm in average) (21). Due to a lower CBCT resolution (0.25 mm voxel size), the PDL layer was not clearly shown in the images. Thus, the root was identified first. The PDL and cortical bone were grown from the surface of the root, see Fig. 1a. The thickness of the PDL and cortical bone was 0.2 mm (22). A bracket, on which the force and moment were applied, was built and attached to the crown, see Fig. 1b. The PDL was modeled as fiber-reinforced matrix, see Fig. 1c. Two nodes link elements were created to connect the nodes on the root and cortical bone surfaces to simulate the fibers (23). Ten-node tetrahedral element was used to model the bone and tooth, see Fig. 1d.

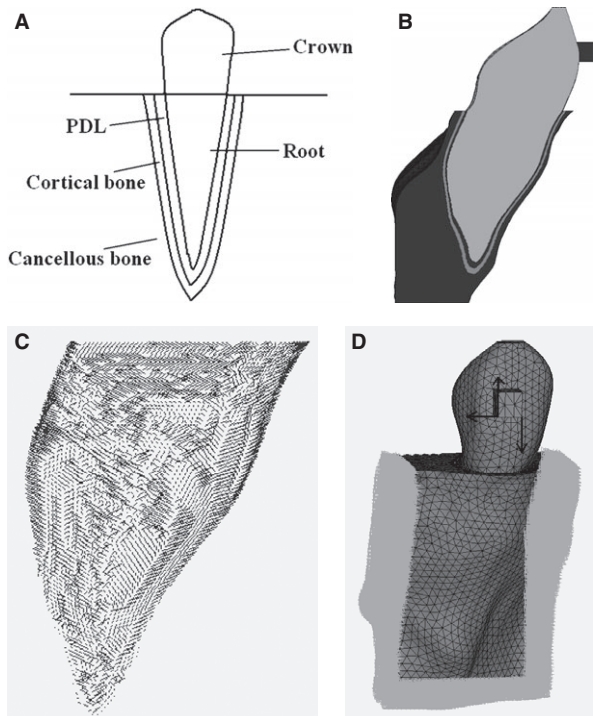


Fig. 1. (A) Schematic diagram of the FE model, (B) Tooth-PDL-bone-bracket model, (C) PDL fiber model, and (D) mesh and boundary/loading conditions. FE, finite element; PDL, periodontal ligament.

A convergence test was performed to determine the minimum element size. Each FE model included approximately 200 000 nodes and 150 000 elements. The material properties reported in literature were assigned (22, 24, 25). Table 1 summarizes the material properties used in the study.

The bottom, mesial, and distal sides of the bone shown in Fig. 1d were fixed. The orthodontic load measured experimentally from the patient was applied to the bracket (17).

The 1st principal, the 3rd principal, von Mises, and dilatational stresses in root, PDL, and alveolar bone were calculated. The root surface, PDL, and cortical bone were represented by three shells. These shells were divided into three vertical levels each with 36 circumferential divisions. Along the canine's long axis, the root from the apex to cervical enamel junction was equally divided into three levels, the apical, middle, and coronal. In the occlusal plane, the shells were divided into 36 divisions circumferentially around the tooth (D1–D36). From the occlusal view, the divisions were labeled counterclockwise for the left canine and clockwise for the right canine with the division in the direction of movement being labeled as D1. The divisions D19 on both canines were opposite to the direction of movement. The divisions D2–D18 were located on the buccal side, whereas D20–D36 on the lingual side. The average values of the four stresses of each division in each level were computed from the FE model. These are the changes in the stresses due to the initial orthodontic

Table 1. Material properties assignment

	Young's modulus	Poisson's ratio	References
Root	18 GPa	0.3	(25)
Cortical bone	13 GPa	0.3	(24)
Cancellous bone	1 GPa	0.3	(24)
PDL	0.5 MPa	0.45	(22)
Fibers in PDL	10 MPa	0.35	(22)
Bracket	200 GPa	0.3	

PDL, periodontal ligament.

Table 2. Interpretations of correlation coefficients

Correlation coefficient range	
$ \mu < 0.5$	Weak correlation
$0.5 < \mu < 0.8$	Moderate correlation
$ \mu > 0.8$	Strong correlation

load. The divisions were made and labeled the same way as were reported in the BMD study (16). This would allow us to compare the stress to the BMD changes. Mixed-model ANOVA was applied to test the correlation between stress and HU change. Correlation coefficient, μ , defined in Table 2 was used to represent the correlations between stress and HU change distribution.

Results

Stress distribution shows the locations of the high and low stresses. Figure 2a, b, c show the dilatational stress distributions in the alveolar bone, PDL, and root surface. The stresses in root were much higher than in the alveolar bone and PDL and were uneven. The stress patterns in the PDL and alveolar bone were significantly different.

The stress distributions of the four types of stress invariants in the 3 by 36 root surface divisions are shown in Fig. 3. The stress distribution was clearly affected by the initial M/F. The major difference occurred at the coronal level. The magnitude of the stress was also very sensitive to the M/F. The M/F close to that for trans-

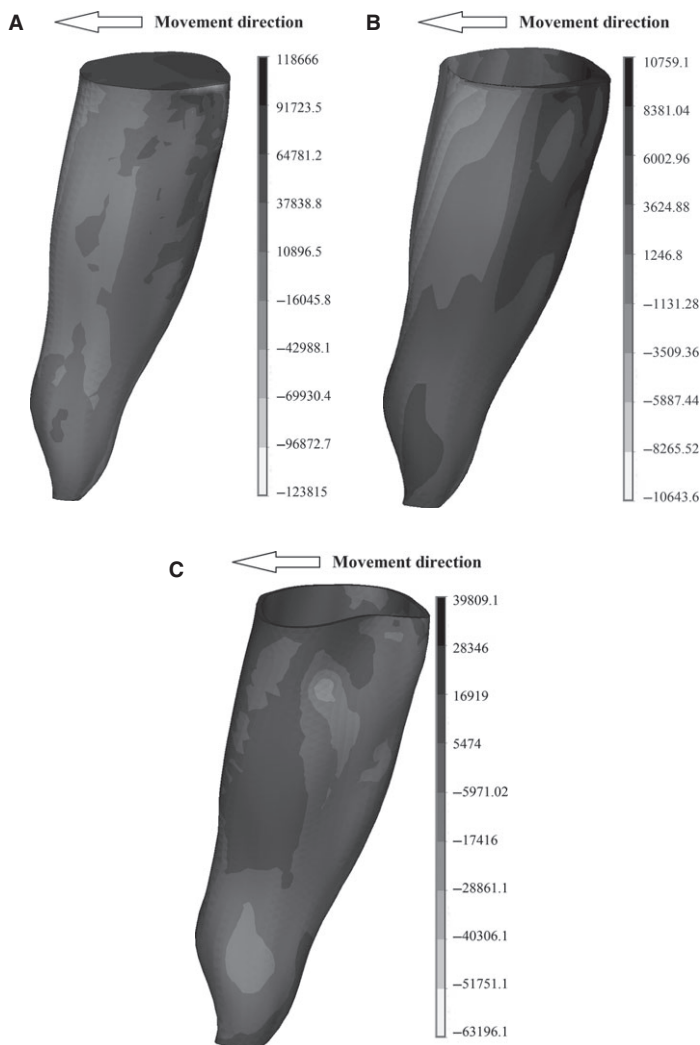


Fig. 2. Dilatational stress distribution in root surface (a), PDL (b), and alveolar bone (c), showing the high stress regions. PDL, periodontal ligament.

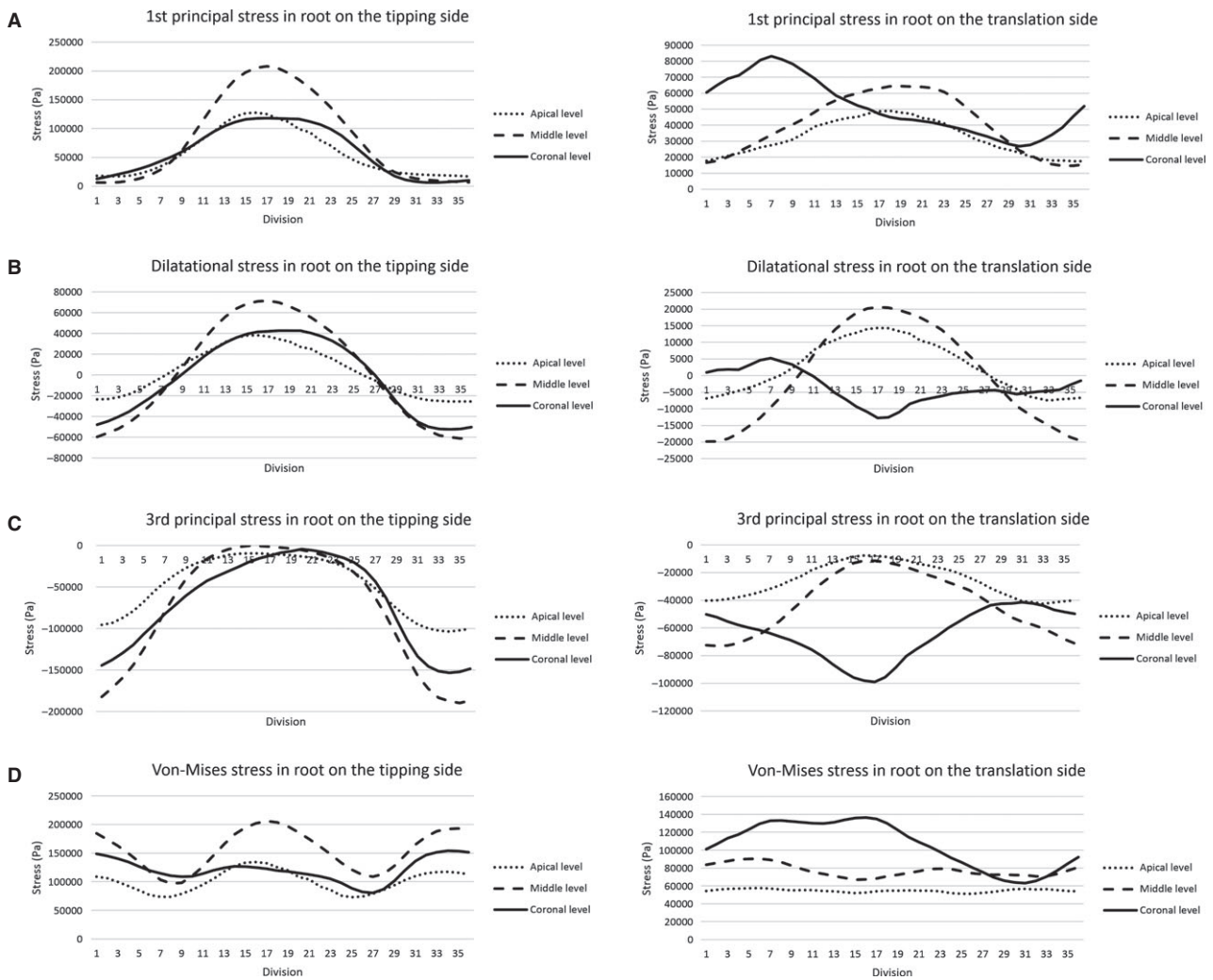


Fig. 3. Stress invariant distributions at the root surfaces in the 3 by 36 root surface divisions corresponding to two treatment strategies, tipping and translation, 1st principal stress (a), dilatational stress (b), 3rd principal stress (c), and von Mises stress (d).

lation resulted in more even stress distribution, with lower stress magnitude and less shear effect characterized by lower von Mises stress. The stress difference between CT and TR side in root was statistically significant.

The stress distributions of the four types of stresses in the PDL divisions are shown in Fig. 4. The stress distributions in PDL corresponding to the tipping and translation strategies were similar, meaning they were less affected by the initial M/F. The stress distributions of the 1st, 3rd principal stress and the dilatational stress were similar. The magnitudes were much lower due to PDL's low Young's Modulus. The stresses were more compressive in the tooth's direction of movement and tension in the opposite direction.

The stress difference between CT and TR side in PDL was not statistically significant overall, but was statistically significant in the direction of movement and the opposite direction.

The stress distribution of the four types of stresses in the alveolar bone divisions are shown in Fig. 5. The stress distributions and magnitudes were similar corresponding to the two treatment strategies, meaning less affected by the M/F. However, the stresses in the alveolar bone showed opposite pattern comparing with these in PDL. The stresses were more tensile on the PDL's compression side and were more compressive in PDL's tension side. The stresses difference between CT and TR side in alveolar bone was not statistically significant.

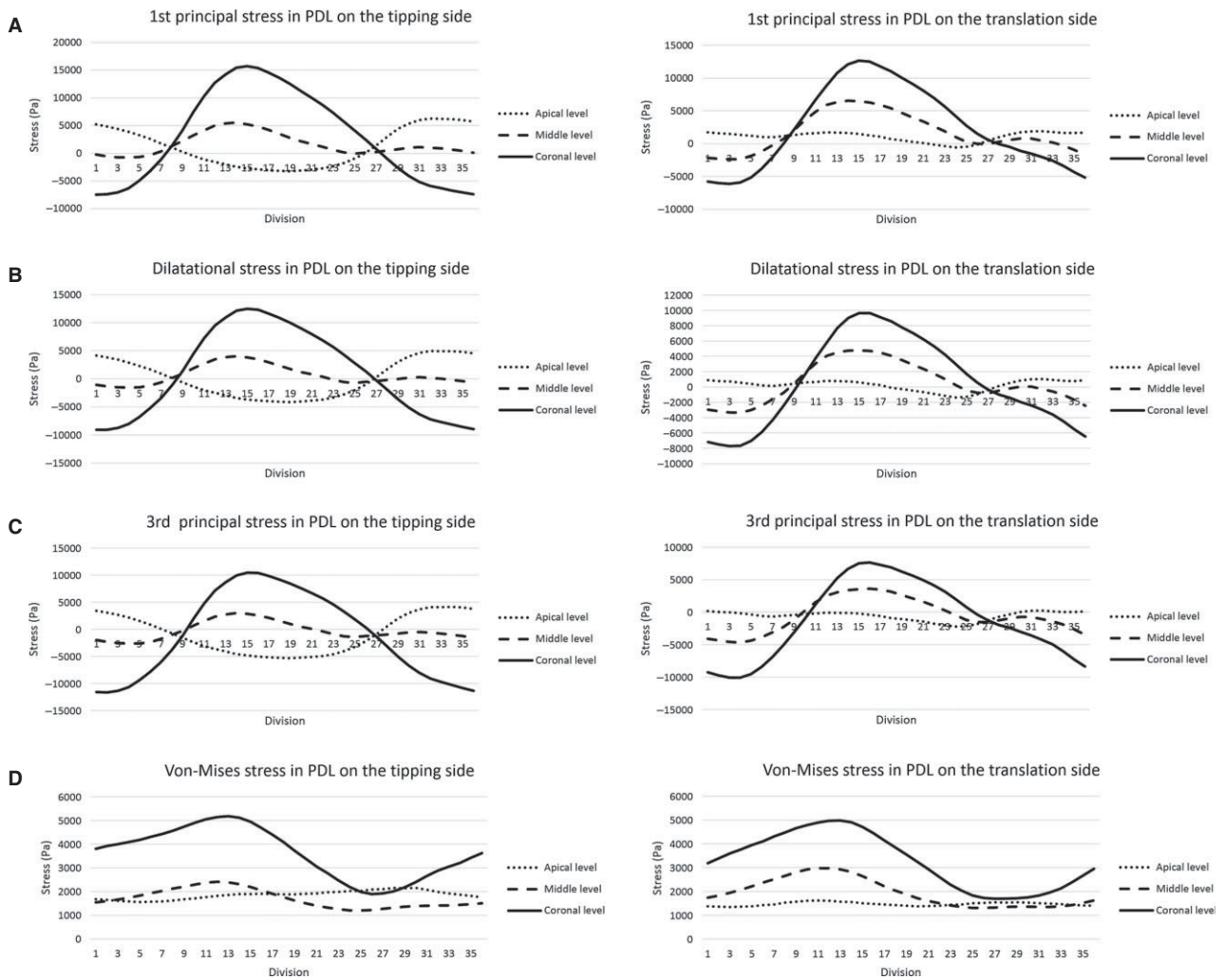


Fig. 4. Stress invariant distributions in the 3 by 36 PDL divisions corresponding to two treatment strategies, tipping and translation, 1st principal stress (a), dilatational stress (b), 3rd principal stress (c), and von Mises stress (d). PDL, periodontal ligament.

Discussion

Only the initial M/Fs were well-controlled. The M/F of a segmental T-loop increased significantly as the canines moved distally so that none of the CT or TR side experienced a constant M/F for translation (17). Therefore, the CT or TR referred here corresponded to the treatment intentions (such as CT or translation) only. Reduction of the M/F increases tipping. Thus, the M/F for CT was lower than TR. Theoretically, an evenly distributed stress occurs if the M/F for translation is applied; as the M/F decreases, the canine tips more distally, which results in uneven stress distributions.

Four stress invariants, 1st principal stress, 3rd principal stress, dilatational stress, and von

Mises stress were reported due to their distinct physical characteristics. The 1st principal stress represents the maximum tensile stress at a point or element in a principal direction (26). The 3rd principal stress shows the maximum compressive stress at a point or element in another principal direction. The dilatational stress characterizes volume change with expansion if positive or ‘squeezing’ if negative. Thus, change of this invariant will force the fluid in the element to flow either in or out. The von Mises stress represents element distortion with no volumetric change. The invariant characterizes shear effect, but will not cause fluid to flow. These are the stress invariants that are unique to the point or element, thus are the preferred parameters for our study. The physical effect

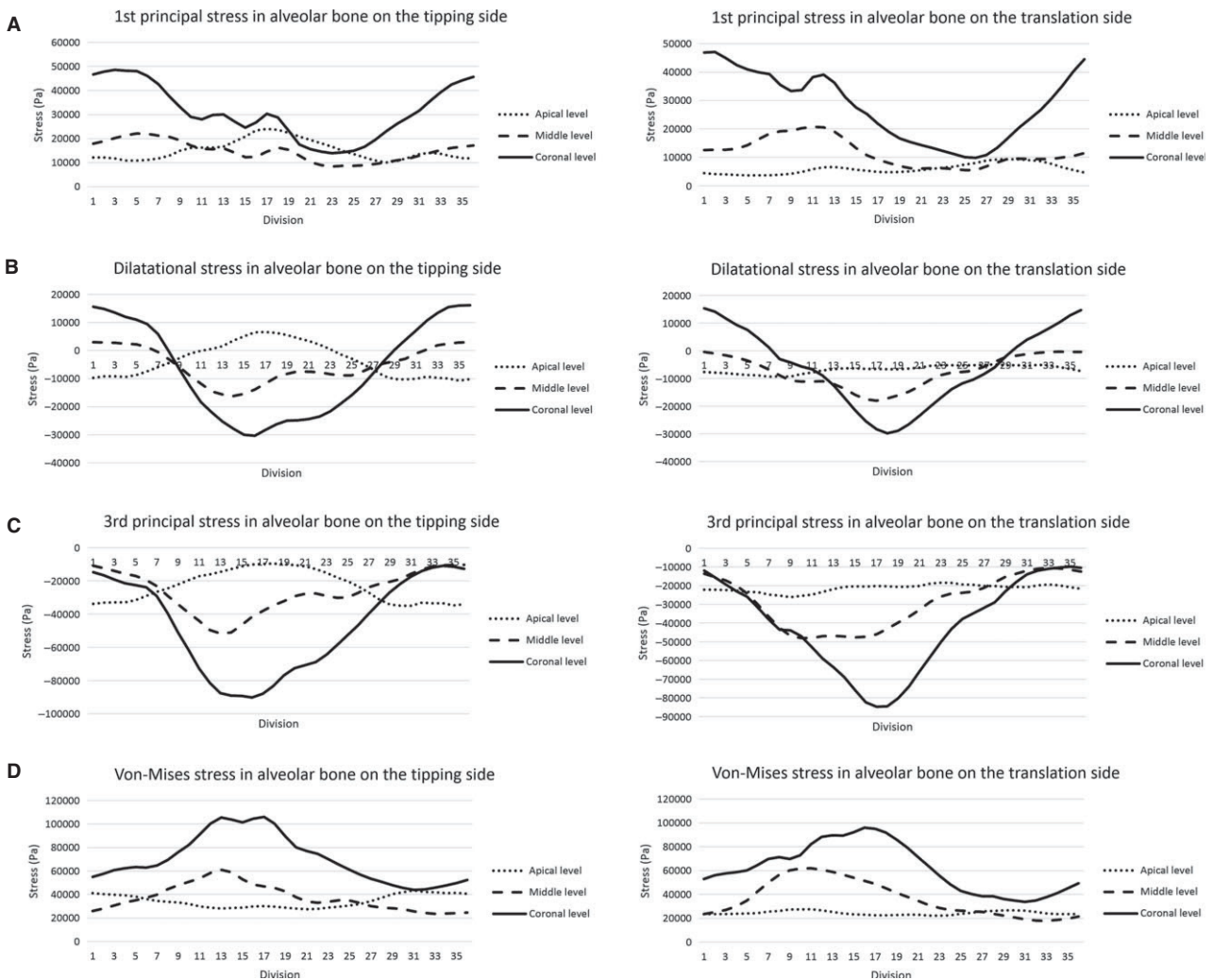


Fig. 5. Stress invariant distributions in the 3 by 36 bone divisions corresponding to two treatment strategies, tipping and translation 1st principal stress (a), dilatational stress (b), 3rd principal stress (c), and von Mises stress (d).

may need to be analyzed based on multiple invariants. A high 1st principal stress and low 3rd principal stress in an element result in more severe stretching than the case where both 1st and 3rd stresses are at the similar level. However, the dilatational stress and von Mises represent volume change and distortion, respectively, which can be used to evaluate their impact on cells directly.

The load on the bracket is transmitted to the alveolar bone through the root and PDL. Our results showed that the stresses in the root were affected the most from the differential M/F, not in the alveolar bone. CT and TR strategies created distinct stress magnitude and distribution patterns, see Fig. 3. The PDL is much softer than the root and the bone. When it was loaded, the

1st principal/dilatational/3rd principal stresses were affected the most, see Fig. 4, squeezing the element on the compression side and expanding the element on the tension side. The stresses then were transmitted to the alveolar bone in a form of more evenly distributed and relatively lower pressure, which resulted in lower stresses in the bone, see Fig. 5. Because of the PDL's buffering effect, the effects of CT and TR strategies diminished, resulting in a similar stress distribution in the alveolar bone.

While the PDL was compressed in front of the moving tooth, the pressure on the cortical shell stretched the bone tangentially. On the other hand, the alveolar bone in the opposite direction was pulled by the PDL fibers, causing the bone to be compressed in the circumferential

direction. Consequently, 1st principal/dilatational/3rd principal stress in PDL and alveolar bone showed reversed patterns. Traditionally, a tooth movement has been described as having a compression and a tension sides. The statement will need to be more specific because it is true only in PDL, not in the alveolar bone.

Investigation of the ME change and its effects on cells helps with understanding the mechanism of mechanotransduction. It is commonly accepted that the bone modeling and remodeling is initially triggered by mechanical load through a mechanotransduction path although the path has not been fully agreed upon. The level of bone activities can be characterized by the change of BMD. Strong bone turnover results in a lower BMD. Thus, it is helpful to see whether the initial ME change in terms of each of the stress invariants is related to the BMD reduction, which may indicate whether certain ME change triggers the bone activities. In this discussion, the BMD were expressed in terms of HU as was reported previously (16).

The four stress invariants changes in the alveolar bone were compared with the HU changes, as seen in Fig. 6. The overall correlations of the stresses with HU changes are generally weak. When data from all directions are combined, none of the correlations were $>|0.5|$. For specific directions, Division 35-3 for CT side showed moderate correlations ($\mu = 0.53-0.61$) between three stress invariants (1st principal/dilatational/3rd principal stress) and HU change in the alveolar bone, meaning the stress and HU change were modest correlated if the comparisons were

along the direction of tooth movement. The stresses in other directions were less changed and were weakly correlated to the HU changes. The level of correlation indicates that the initial stress may not be the only stimulus that determines the HU changes. Patient-specific biological responses may also be major factors.

To better understand the relationship, the dilatational stress at the coronal level was compared with the corresponding BMD changes, see Fig. 6. The results showed that the high dilatational stress area in the bone in the direction of tooth movement had high HU reduction, indicating high remodeling. This stress indicates volume expansion, meaning less pressure on the osteocytes. The area corresponds to bone resorption; thus, the pressure reduction may be related to osteoclast recruitment. The low dilatational stress in the bone in the opposite direction also had high HU reduction, indicating high remodeling. The stress indicate volume reduction, meaning squeezing the cells. The area corresponds to bone deposition, thus increasing pressure on the cells may be related to osteoblast recruitment. This explanation is in agreement with the traditional orthopedic view that bone is generated under compression and resorbed under tension (27–29). It also supports reports from other studies (6, 9–11) that the osteocyte senses the mechanical stimuli and releases signaling molecules to regulate osteoblasts and osteoclasts. The potential mechanisms are due to unloading of osteocyte for producing more osteoclasts (30) and loading or increasing strain-driven fluid flow for producing more osteoblasts (31).

How osteocytes sense the load as the mechanosensing cells has been studied. Substrate strain, fluid shear stress, and the loading-induced hydraulic pressure are potential mechanical stimulus for osteocytes (8, 32). This study has provided evidence that the area that has high volumetric change has more HU reduction, meaning more modeling/remodeling activities. The change affects both strain and extracellular fluid flow, which provides the needed stimuli.

It had been reported previously that no significant difference of BMD change patterns had

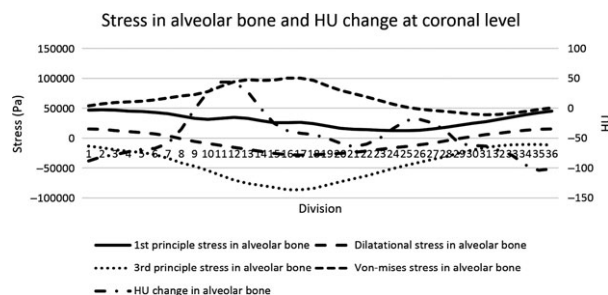


Fig. 6. Comparison of stresses and Hounsfield Unit (HU) change in the 36 alveolar bone divisions at the coronal level. High dilatational stress area in the bone in the direction of tooth movement and low in the opposite direction had high HU reduction, indicating high remodeling.

been detected in the surrounding alveolar bone under the two treatment strategies (16). This is in agreement with our stress analysis. Due to the buffering effect, the stress in bone was minimally affected by the M/F, which may be the reason that BMD change was not related to M/F as well.

Conclusions

The stress invariants can be used to characterize how the osteocytes are affected when ME changes.

The stress invariants' distributions in bone, PDL, and root are significantly different, meaning the cells in the tissues experience different stimuli.

The stress invariants in the alveolar bone are not significantly affected by different M/F.

The higher bone modeling/remodeling activities along the direction of tooth movement may be related to the initial volumetric increase and decrease in the alveolar bone.

Clinical relevance

This study supports that osteocyte is responsible for regulating bone modeling/remodeling and reveals the effects of different T-loop designs on the ME changes in the root, PDL, and the alveolar bone. If the osteocyte is responsible to regulate bone modeling/remodeling activities, changing M/F would have limited effects on osteocyte stimulation.

Acknowledgement: This research was supported by the NIH/NIDCR under grant no. 1R01DE018668.

References

1. Wise GE, King GJ. Mechanisms of tooth eruption and orthodontic tooth movement. *J Dent Res* 2008;87:414–34.
2. Roberts-Harry D, Sandy J. Orthodontics. Part 11: orthodontic tooth movement. *Br Dent J* 2004;196:391–4; quiz 426.
3. Rody WJ Jr, King GJ, Gu G. Osteoclast recruitment to sites of compression in orthodontic tooth movement. *Am J Orthod Dentofacial Orthop* 2001;120:477–89.
4. Onal M, Xiong J, Chen X, Thosten-JD, Almeida M, Manolagas SC et al. Receptor activator of nuclear factor kappaB ligand (RANKL) protein expression by B lymphocytes contributes to ovariectomy-induced bone loss. *J Biol Chem* 2012;287:29851–60.
5. Vezeridis PS, Semeins CM, Chen Q, Klein-Nulend J. Osteocytes subjected to pulsating fluid flow regulate osteoblast proliferation and differentiation. *Biochem Biophys Res Commun* 2006;348:1082–8.
6. You L, Temiyasathit S, Lee P, Kim CH, Tummala P, Yao W et al. Osteocytes as mechanosensors in the inhibition of bone resorption due to mechanical loading. *Bone* 2008;42:172–9.
7. Bonewald LF. The amazing osteocyte. *J Bone Miner Res* 2011;26:229–38.
8. Klein-Nulend J, Bacabac RG, Bakker AD. Mechanical loading and how it affects bone cells: the role of the osteocyte cytoskeleton in maintaining our skeleton. *Eur Cell Mater* 2012;24:278–91.
9. Robling AG, Bellido T, Turner CH. Mechanical stimulation in vivo reduces osteocyte expression of sclerostin. *J Musculoskelet Neuronal Interact* 2006;6:354.
10. Santos A, Bakker AD, Zandieh-Doulabi B, Semeins CM, Klein-Nulend J. Pulsating fluid flow modulates gene expression of proteins involved in Wnt signaling pathways in osteocytes. *J Orthop Res* 2009;27:1280–7.
11. Tan SD, de Vries TJ, Kuijpers-Jagtman AM, Semeins CM, Everts V, Klein-Nulend J. Osteocytes subjected to fluid flow inhibit osteoclast formation and bone resorption. *Bone* 2007;41:745–51.
12. Barbagallo LJ, Jones AS, Petocz P, Darendeliler MA. Physical properties of root cementum: part 10. Comparison of the effects of invisible removable thermoplastic appliances with light and heavy orthodontic forces on premolar cementum. A microcomputed-tomography study. *Am J Orthod Dentofacial Orthop* 2008;133:218–27.
13. Chan EK, Darendeliler MA. Exploring the third dimension in root resorption. *Orthod Craniofac Res* 2004;7:64–70.
14. Viecilli RF, Katona TR, Chen J, Hartsfield JK Jr, Roberts WE. Orthodontic mechanotransduction and the role of the P2X7 receptor. *Am J Orthod Dentofacial Orthop* 2009;135:694.e1–16; discussion 94–5.
15. Chang HW, Huang HL, Yu JH, Hsu JT, Li YF, Wu YF. Effects of orthodontic tooth movement on alveolar bone density. *Clin Oral Invest* 2012;16:679–88.
16. Jiang F, Liu SY, Li S, Xia Z, Kula K, Eckert G et al. Hounsfield unit change in root and alveolar bone during canine retraction. *Am J Orthod Dentofac Orthop* in press.
17. Xia Z, Chen J, Jiang F, Li S, Viecilli RF, Liu SY. Load system of segmental T-loops for canine retraction. *Am J Orthod Dentofac Orthop* 2013;144:548–56.
18. Li S, Xia Z, Shih-Yao S, Eckert G, Chen J. Three-dimensional canine displacement patterns in response to translation and controlled tipping

- retraction strategies. *Angle Orthod* 2015;85:18–25.
19. Bath-Balogh M, Fehrenbach M. *Illustrated Dental Embryology, Histology, and Anatomy, 3rd edn*. St. Louis, MO: Elsevier Saunders; 2011.
 20. Auyeung L, Bouwsma OJ, Polson AM. Periodontal fiber attachment and apical root resorption. *Endod Dent Traumatol* 1988;4:219–25.
 21. Cawson RA, Odell EW. *Cawson's Essentials of Oral Pathology and Oral Medicine*. Edinburgh, USA: Churchill Livingstone; 2008.
 22. Qian H, Chen J, Katona TR. The influence of PDL principal fibers in a 3-dimensional analysis of orthodontic tooth movement. *Am J Orthod Dentofac Orthop* 2001;120: 272–9.
 23. Meyer BN, Chen J, Katona TR. Does the center of resistance depend on the direction of tooth movement? *Am J Orthod Dentofac Orthop* 2010;137:354–61.
 24. O'Grady J, Sheriff M, Likeman P. A finite element analysis of a mandibular canine as a denture abutment. *Eur J Prosthodont Restor Dent* 1996;4:117–21.
 25. Katona TR, Paydar NH, Akay HU, Roberts WE. Stress analysis of bone modeling response to rat molar orthodontics. *J Biomech* 1995;28: 27–38.
 26. Ugural AC, Fenster SK. *Advanced Strength and Applied Elasticity*, 4th edn. Upper Saddle River, NJ: Prentice Hall PTR; 2003.
 27. Currey J. *The Mechanical Adaptations of Bones*. Princeton, NJ: Princeton University Press; 1984.
 28. Martin RB, Burr DB. *Structure, Function, and Adaptation of Compact Bone*. New York, NY: Raven Press; 1989.
 29. Jansen M. *On Bone Formation: Its Relation to Tension and Pressure*. London: Longmans; 1920.
 30. Tatsumi S, Ishii K, Amizuka N, Li M, Kobayashi T, Kohno K et al. Targeted ablation of osteocytes induces osteoporosis with defective mechanotransduction. *Cell Metab* 2007;5:464–75.
 31. Robinson JA, Chatterjee-Kishore M, Yaworsky PJ, Cullen DM, Zhao W, Li C et al. Wnt/beta-catenin signaling is a normal physiological response to mechanical loading in bone. *J Biol Chem* 2006;281: 31720–8.
 32. Price C, Zhou X, Li W, Wang L. Real-time measurement of solute transport within the lacunar-canalicular system of mechanically loaded bone: direct evidence for load-induced fluid flow. *J Bone Miner Res* 2011;26: 277–85.

Copyright of Orthodontics & Craniofacial Research is the property of Wiley-Blackwell and its content may not be copied or emailed to multiple sites or posted to a listserv without the copyright holder's express written permission. However, users may print, download, or email articles for individual use.